2-D Simulation of Flow Structures Over Dunes for Flow Characteristics Estimation

Mohammad Sharifi
Shahid Beheshti University

Mohammad Reza Majdzadeh Tabatabai
Shahid Beheshti University, m_majdzadeh@sbu.ac.ir

Seyed Hossein Ghoreishi Najafabadi
Shahid Beheshti University

Recommended Citation

Sharifi M., Majdzadeh Tabatabai, M.R., and Ghoreishi Najafabadi, S.H. (2022). "2-D Simulation of Flow Structures Over Dunes for Flow Characteristics Estimation" in "9th IAHR International Symposium on Hydraulic Structures (9th ISHS)". *Proceedings of the 9th IAHR International Symposium on Hydraulic Structures – 9th ISHS*, 24-27 October 2022, IIT Roorkee, Roorkee, India. Palermo, Ahmad, Crookston, and Erpicum Editors. Utah State University, Logan, Utah, USA, 11 pages (DOI: 10.26077/f04b-f7cd) (ISBN 978-1-958416-07-5).

9th International Symposium on Hydraulic Structures Roorkee, India 24-27 October 2022
ISBN: 978-1-958416-07-5 DOI: https://doi.org/10.26077/f04b-f7cd

2-D simulation of flow structures over dunes for flow characteristics estimation

Mohammad Sharifi[1], Mohammad Reza Majdzadeh Tabatabai[2], Seyed Hossein Ghoreishi Najafabadi[2]
[1]*PhD Candidate, Department of Civil, Water and Environmental Engineering, Shahid Beheshti University, Tehran, Iran*
[2]*Assistant Professor, Department of Civil, Water and Environmental Engineering, Shahid Beheshti University, Tehran, Iran*
E-mail: m_majdzadeh@sbu.ac.ir

Abstract: *Rivers have undulated beds, which are called bedforms. Depending on the hydraulic conditions, the bedforms have different types that cause resistance in the flow. Despite various research and experiments on bedforms, the topic is still debatable and requires further research. The present study is mainly focused on simulating the flow motion numerically on dunes in open channels to evaluate the effect of dune geometry on flow structure. Twenty-nine simulations were conducted to study the effect of the geometry of five types of dunes with different angles and heights under different hydraulic conditions and bed roughnesses. RANS and DES turbulence models were used to simulate small and large-scale dunes, respectively. The results of the numerical model were compared with the experimental results of previous researchers to validate the work, indicating the appropriate accuracy of the numerical model. Then, an empirical equation was adopted to evaluate the effect of dune geometry on flow hydraulics by considering the equations of previous researchers. Finally, sensitivity analyses were carried out to determine the dependence of each parameter in this equation.*

Keywords: *Bedform, Dune, Numerical simulation, Turbulence models.*

1. Introduction

Generally, rivers play a crucial impact on their surrounding areas and are considered a crucial water supply source for humans. Therefore, any changes in the river flow regime could disturb the social-economic of the riparian zone and endanger their lives. In open channel flow with a fixed bed, it is possible to estimate a constant value to determine the roughness coefficient (Ahmad *et al.* 2017, Chow 1981) and use one of the flow resistance formulas to calculate the flow rate (Fenton 2010). In natural rivers with alluvial beds, bed deformation may occur with the entrainment of particles, which could be followed by bedforms, depending upon the flow conditions. The bed deformation could increase the hydraulic flow resistance, which may result in the particles (Strickler 1923, Aberle et al. 2008, Ji-Sung, et al. 2010) and bedforms roughness (Engelund and Hansen 1967, Hafez *et al.* 2001, Venditi 2007). Although various researchers have used different approaches to estimate the bedforms (Heydari *et al.* 2014, Attar and Li 2012, Karamisheva *et al.* 2005 and Julien and Klaassen 1995), their results are significantly different. This could be owing to the differences in laboratory conditions, lack of uniformity to predict bedform dimensions and the shortage of knowledge about the effect of bedform structure on the turbulence of sediment transport phenomena. This, in turn, necessitates further research on the complexity of the phenomena.

Many researchers have noticed the significant effect of the bedforms on the flow structure, by decomposing the total roughness into grain and form roughnesses (Cai *et al.* 2020). The term “dune” was initially introduced by Gilbert (1914). Soulsby (1989) suggested that a triangular, asymmetrical cross-sectional area generally forms sand waves with a sharp lee-side angle of 28 to 35° and a gentle stoss-side angle of about 5°. Dunes cause a flow separation zone at the lee-side, in which eddy flows are formed and dissipate much energy. By measuring the velocity in this zone, he observed that the velocity is approximately one-third to half of the average flow velocity in the stoss-side direction.

Giri and Shimizu (2006) presented a two-dimensional morphodynamic model for free surface flows on bedforms. The proposed model has a high ability to simulate average flow and turbulence structure. They validated the model with laboratory data in a mobile bed channel and compared it with previous works. They also found that the nonlinear $k-\varepsilon$ model showed better results than the linear model, particularly, in turbulent zones. Nabi et al. (2012) presented a three-dimensional high-resolution hydrodynamic model for unsteady incompressible flow over an evolving bed topography. The model used LES to solve the turbulence; their results were compared with the laboratory and experimental models of previous research works and showed reasonable agreement. Reisenbüchler *et al.* (2019) cited that Van Rijn (1984c) developed a diagram, based on a large number of laboratory and field data, to determine the bedform in open channels. Niazkar *et al.* (2019) developed a direct flow-dependent approach

calculating roughness caused by the grain and bedform. They compared the accuracy of their method with the previous works.

In general, experimental studies to evaluate the effect of bedforms on flow structure is costly and time-consuming. At the same time, numerical studies provide additional information and reduce time and cost. Motamedi *et al.* (2012) investigated the length of the separation zone and the interaction of dune geometry on the flow structure. They concluded that the length of the flow separation zone could increase directly with the flow rate, dune height and bed material size, and decrease inversely with the flow depth. Lefebvre (2019) used Delft3D software to simulate 3D flow above natural bedforms. He initially verified the model against Maddux *et al.* (2003) laboratory data. Then, Parsons *et al.* (2005) data were used to model 3D flow velocities and turbulence above a dunes bedform field for Río Paraná (Argentina).

Although many research works have been undertaken on the resistance of dunes to the flow, the topic is still debatable as this signifies the necessity of further research on the dune geometry and its effect on flow structure. Furthermore, assessment of an appropriate turbulence model is of great importance to simulate the geometry of the bedforms under different hydraulic conditions.

In this regard, adapting empirical equations to estimate dunes dimensions enables us to gain a better understanding of the interaction between bedforms and flow structure. Generally, most previous research works used the Reynolds-averaged Navier–Stokes (RANS) turbulence model to simulate the flow structure because of its simplicity and low cost (Berrouk 2019). However, on account of its deficiency in computing velocity fluctuations, the model fails to detect accurately flow eddies (Spalart and Allmaras 1994 and Spalart *et al.* 1997) and leads to an inappropriate demonstration of flow separation at the dunes lee side. Hence, this study used the detached eddy simulation (DES) turbulence model in STAR-CCM+ to simulate flow on large-scale dunes (i. e. dune height to water depth ratio of greater than 0.25) with a high lee-side angle (38°), as the effect of the bedforms on the flow structure is significant in a shallow-water river. In contrast, the significance of bedform roughness decreases by increasing the ratio of water depth to dune height, which may reflect the flow separation formation at the dune lee-side (Mustaffa *et al.* 2016). Since riverbed conditions are one of the factors affecting floods and aquatic life cycles, this study attempts to identify the effective parameters on the bedforms to obtain an in-depth understanding of the interaction between them and the flow structure to be applied to the river by the engineers and practitioners. Besides, further efforts have been made to develop an empirical equation to predict the interaction of riverbed geometry and flow characteristics.

2. Methods

2.1. Governing equations

The flow of a viscous incompressible fluid with constant properties is governed by the Navier–Stokes equations (Alfonsi 2009):

$$\frac{\partial u_i}{\partial t} + \frac{\partial}{\partial x_j}\left(u_i u_j\right) = -\frac{\partial p}{\partial x_i} + \nu \frac{\partial^2 u_i}{\partial x_j \partial x_j}, \frac{\partial u_i}{\partial x_i} = 0 \qquad (1)$$

The Reynolds equation, which is called RANS, is one of the Navier-Stokes equations, where u = velocity, x = location, t = time, i and j = Cartesian indices, P = pressure, and ν = kinematic viscosity of water. According to the concept of Reynolds decomposition, the dependent variables of equation (1) decomposed into mean and fluctuating parts:

$$u_i = \bar{u}_i + u_i', \quad p = \bar{p} + p' \qquad (2)$$

Where the sign ($'$) = the fluctuating component while the sign ($\bar{\ }$) = the time average component (Alfonsi 2009). The left-hand side of equation (1) represents the changes in the mean momentum caused by the unsteady flow and convective accelerations. It is notable that the term $\frac{\partial}{\partial t}$is eliminated when the flow is steady.

2.2. Numerical setup

Sharifi et al. (2020) suggested that DES and RANS turbulence models give the most appropriate results for large and small-scale dunes, respectively. Star-CCM+ was applied as the tool to carry out the simulation. It is a state-of-the-art commercial code developed by CD-Adapco (Melville, New York, USA) which solves the fully 3-D hydrodynamic incompressible Navier–Stokes equations using a finite volume method on unstructured meshes (Wu *et al.* 2019). The realizable two-layer k-ε model was used to perform the RANS simulations. Based on previous studies (Shur *et al.* 1999, Bunge *et al.* 2007, Spalart *et al.* 1997), the k-ε model was applied as a principle for the RANS model in DES, which the constant is shown is Table 1. The no-slip condition was considered for bed and side walls while the layer of air with height equals twice the water depth was added to the computational

domain to model free surface dynamics using the VOF. Furthermore, the volume of fraction method was applied to calculate the free surface. The numerical solution method in this model is implicit unsteady. The VOF method has been used for problems involving two or more unmixable fluids and the interface between the two fluids (Park *et al.* 2020). A simple but powerful method is described based on the concept of a fractional volume of fluid (VOF). This method is more flexible and efficient than other methods for treating complicated free boundary configurations (Hirt *et al.* 1981). By solving these equations, the number α is obtained to indicate the volumetric ratio of the two fluid phases within each of the computational cells. For example, $\alpha = 1$ indicates that the cell volume is full of water, $\alpha = 0$ shows that the cell volume is full of air, and $0 < \alpha < 1$ is the transition zone between the two water and air fluids. For an incompressible fluid, the kinematic volume fraction; is:

$$\frac{\partial F}{\partial t} + \frac{1}{V_F}\left[\frac{\partial (F A_i u_i)}{\partial x_i}\right] = \frac{1}{V_F}\left[\frac{\partial \left(\upsilon_F A_i \partial F / \partial x_i\right)}{\partial x_i}\right] \quad (3)$$

Where u_i = horizontal component of velocity; x_i = horizontal vector in the Cartesian coordinate system; V_F = volume fraction of fluid in each cell; A_i = fractional areas open to flow in the i-coordinate of the Cartesian system; υ_F = diffusion coefficient and F = the volume of fluid per unit volume (User Guide, STAR-CCM+ 2018).

Table 1. Constants of k-ε model

C_μ	$C_{\varepsilon 1}$	$C_{\varepsilon 2}$	σ_k	σ_ε
0.09	1.44	1.9	1	1.2

2.3. Experimental data

The laboratory model developed by Motamedi *et al.* (2012) was used to simulate the flow on dune bedforms. They conducted their experiments in a rectangular channel 12 m long, 0.75 m wide and 0.9 m high on fixed dunes with different dimensions and lee and stoss-side angles (Nelson *et al.* 1993, Allen 1985, Nasiri 2010 and Davarpanah 2011). The material of dunes was of two types of non-uniform sand with an average diameter of 5.8 and 13.2 mm, which were referred to as fine and coarse grains, respectively, in this research. The dunes had a wavelength of 1 m and heights of 4, 6, and 8 cm, which were divided into sharp and flat-crested classes. The former were of type 2 (Figure 1, Table 2) while the latter were of type 1, 3 and 4 (Figure 1, Table 2). Dune type 3 was a large-scale dune with a height to water depth ratio greater than 0.25 and a lee-side angle of 38°. However, other dunes were of the small-scale type with a height to water depth ratio of less than 0.25 and the lee-side angle less than 38°.

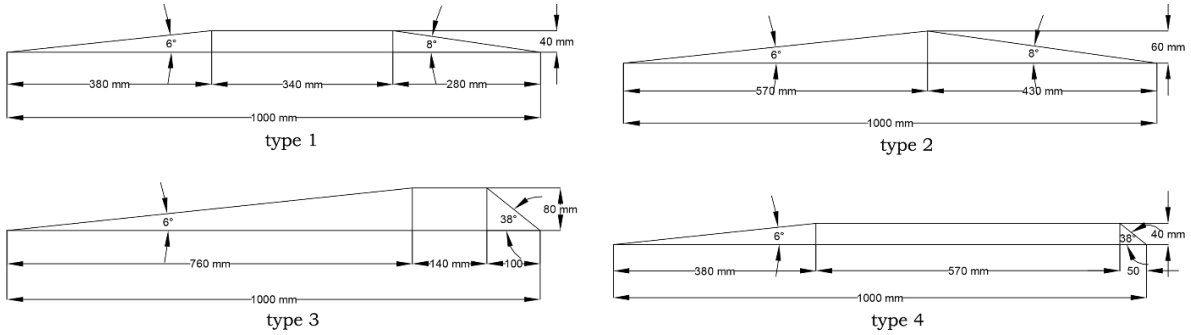

Figure 1. Used sharp-crested dune (type 2) and Used broad-crested dune (type 1, 3 and 4) (Motamedi et al. 2012)

The experiments were carried out with discharge values of 30 and 60 litres per second under depths of 32 and 20 cm (Motamedi *et al.* 2012). In addition, Balachandar and Patel (2008) data were also used to simulate the flow on the dune bedform; they applied Van Mierlo and de Ruiter (1988) dune geometry (Figure 2, Table 2) and created a train of 22 dunes in a laboratory channel with dimensions of 10 m long, 0.61 m wide and 0.61 m high. Experiments were conducted under the constant velocity of 0.4 m/s and the flow depth of 0.12 m (Balachandar and Patel 2008). They consider three modes of flat bed, the bed covered with a network of 0.72 mm stainless steel wires with a distance of 6.35 mm and bed glued with 18 mm sand grains, which was simulated in the present study.

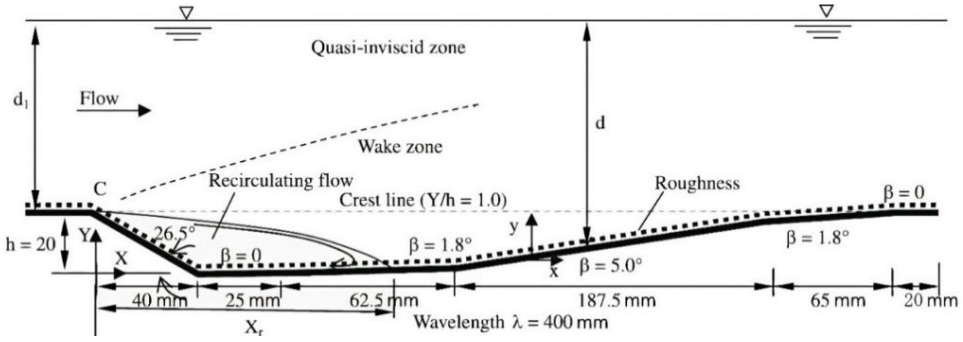

Figure 2. Experimental model of dune geometry (Balachandar and Patel 2008)

Table 2. Characteristics of geometry dimensions of simulated dunes

Dune length	Stoss side angle (Degree)	Crest length (cm)	Dune height (cm)	Lee side angle (Degree)	Crest type	Dune type
100	6	0	6	8	Sharp	2
100	6	34	4	8	Broad	1
100	6	14	8	38	Broad	3
100	6	57	4	38	Broad	4
40	5	2	2	26.5	Broad	Balachandar

2.4. Boundary conditions

The numerical model was designed with input and output boundary conditions in which “Velocity Inlet” option with constant velocity was selected in Star-CCM+ for the input boundary condition. For the output boundary condition, "Pressure Outlet" option was selected equal to nought, likewise, for the free water surface to address the effect of the atmosphere. The walls and bed of the channel were also considered with the “Wall” option; this was determined by equivalent roughness k_s to be $2.5D_{50}$and $3.5D_{84}$(Yang *et al.* 2005 and Motamedi *et al.* 2012) for the fine and coarse materials, respectively (Figure 3). The flow of water was assumed incompressible with a density of $1000\ kg/m^3$ and dynamic viscosity of $0.001\frac{kg}{m.s}$.

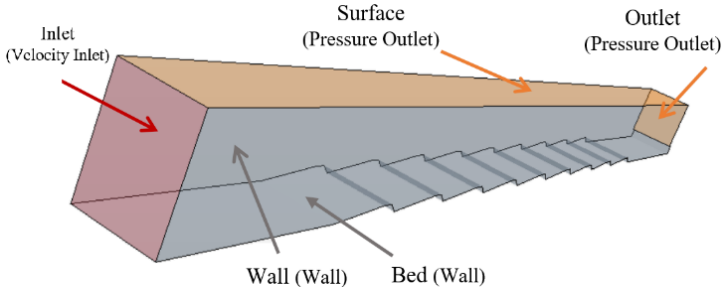

Figure 3. Numerical model boundary conditions in STAR-CCM + software

2.5. Mesh Generation

In general, selecting the most optimal mesh size is regarded as one of the most critical steps in numerical simulation. As coarse meshing increases, the gradient of variables variations as a result of which inappropriate outputs may be gained. Hence, fine meshing should be implemented so that all cases can be examined by condensing the mesh points in the zones where the flow variables are under sudden changes. Therefore, it enables us to achieve outputs more accurately by studying all the model variables in a computational domain. Nevertheless, should fining mesh sizes be performed with caution. This is because it would increase the number of computational cells and the extension of computational time, which may not be economical. By this means, mesh optimization should initially be implemented in numerical simulation.

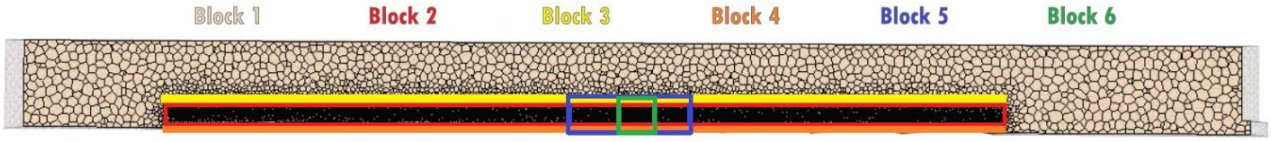

Figure 4. Meshing blocks

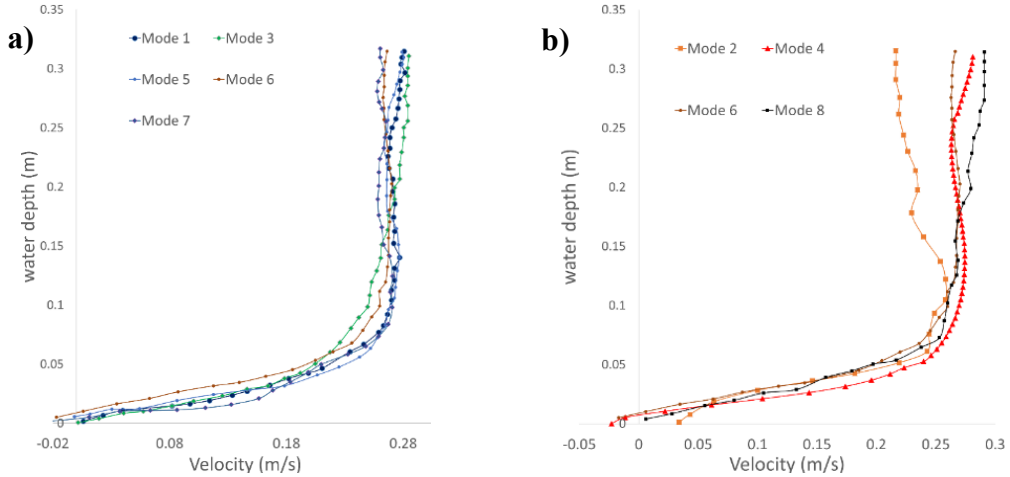

Figure 5. Profile changes velocity in the vertical direction. a) Couple states and b) odd states relative to the ideal state (6)

For example, simulation No. 25 (Dune type 4, 58 mm grain size, 30 l/s flow rate and 317 mm flow depth) was chosen arbitrarily for the optimal cell size selection tests. To measure the sensitivity of the numerical model to the computational cell size, as well as to optimize the run time and to promote the accuracy of the outputs, changes in the meshing size were considered in the form of multiple blocks in the sampling data locations on the dunes (Figure 4). Eight simulations were carried out to optimize the time and accuracy of the output results. Based on this, the model with the smallest cell size (i. e. mesh generation mode (6) was selected as the most accurate (100%) under a long run time of 98 hours. Given, the run time was not cost-effective; however, accuracy was desirable. Thus, other modes were validated by this in terms of velocity profile deviation in the vertical direction (Figure 5 and Table 3). Under these circumstances, mesh generation mode (1) worked out having optimized simulation with appropriate accuracy of 85% under a run time of 50 hours. It is worth pointing out that no significant change is observed in the accuracy of the model by reducing the mesh sizes. however, the run time increases significantly to reach stable time (Section 2-7). Equally, enlarging the mesh sizes could significantly increase the deviation of the vertical velocity profile (Figures 5a and b) and, subsequently, the divergence of the streamlines and further mixing of the water and air (Figures 6a and b). Hence, the mesh dimensions mode (1) is selected as the appropriate option (Figure 7). The average value of GCI is 1.025 approximately.

Table 3. Mesh generation sensitivity analyses

Mesh Generation Mode	Dimensions of grid in block 1 (mm)	Dimensions of grid in block 2 (mm)	Dimensions of grid in block 3 (mm)	Dimensions of grid in block 4 (mm)	Dimensions of grid in block 5 (mm)	Dimensions of grid in block 6 (mm)	Time required to sec in reach 60 simulation time (hour)	Percentage of flow deviation
1	100	20	10	20	10	5	50	15
2	100	40	20	20	10	5	40	27
3	100	20	10	5	10	5	66	13
4	100	20	10	10	10	1	82	9
5	100	20	10	10	10	2	74	11
6	100	20	10	10	5	1	98	8
7	100	20	10	10	5	5	61	14
8	100	20	10	10	10	5	55	15

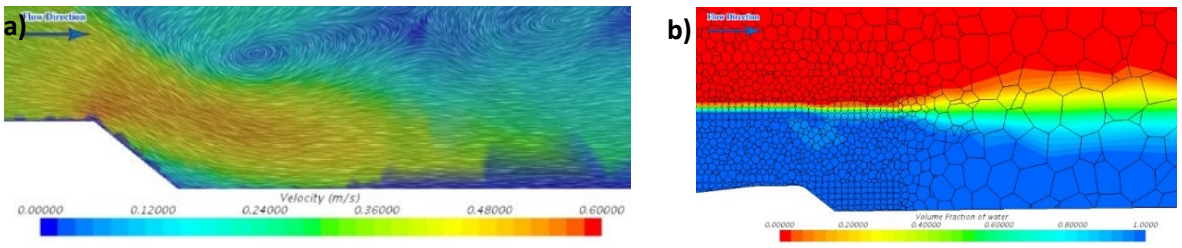

Figure 6. Distribution a) Streamlines and b) Mixing the weather in the vicinity of the last telescope with a large meshing of 10 cm

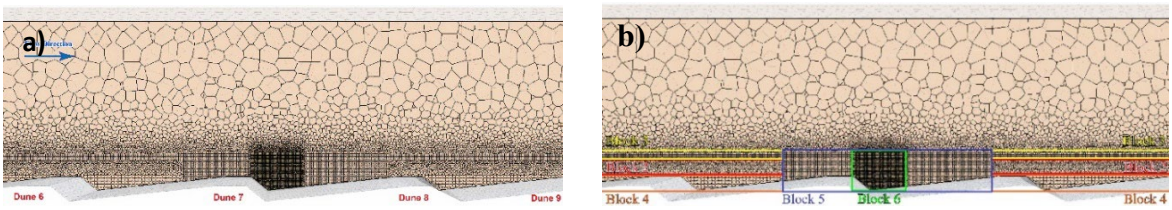

Figure 7. The meshing of numerical model sampling location a) Overview b) Location of blocks

2.6. Time of equilibrium

Time of equilibrium or stability time of the numerical model may vary depending upon the dimensions of the mesh sizes and the applied turbulence model. The accuracy of the simulation results is directly related to the run time of the model which may not be economical for a long run time. When the simulation accuracy reaches about 80 to 90% of its final value after a certain time, it could be accepted as the final result to save time and money.

In this way, experiments were carried out finding the optimal run time for numerical simulation. On account of the different simulation times for each turbulence model, two experiments were made with two different geometries under various hydraulic conditions, one of which with the RANS turbulence model (simulation No. 24 (Dune type 4, 132 mm grain size, 60 l/s flow rate and 195 mm flow depth)) and the other with the DES turbulence model (simulation No. 17 (Dune type 3, 132 mm grain size, 60 l/s flow rate and 317 mm flow depth)). Since RANS equations are based on time-averaged approach, these equations have fewer computational processes and their run time is shorter than that of the DES model. The model was run for 40, 50, 60, 70, 80, and 90 seconds to simulate the RANS model, and the velocity profiles were compared at the boundary between the fifth and sixth dunes (Figures 8a and b). The model has achieved acceptable accuracy from the very first seconds, enabling us to select the run time of 50 seconds as the stability time to achieve sufficient accuracy in the simulations of the RANS.

The run times of 40, 50, 60, 70, 80, and 90 seconds were made in the numerical model to find the optimal simulation time for the DES, and then, the velocity profiles were compared the same as before for the same location. Figure (8b) indicates that the velocity profiles differ by less than 7% in 60 and 70 seconds, therefore, the DES requires more time to achieve sufficient accuracy, which takes the run time of about 60 seconds. However, for more certainty, the run time of 70 seconds was selected for simulation to ensure that the process was appropriately in progress. The times obtained in the process can be considered as the time for the flow to reach stability because no significant differences have been noticed in the velocity profiles.

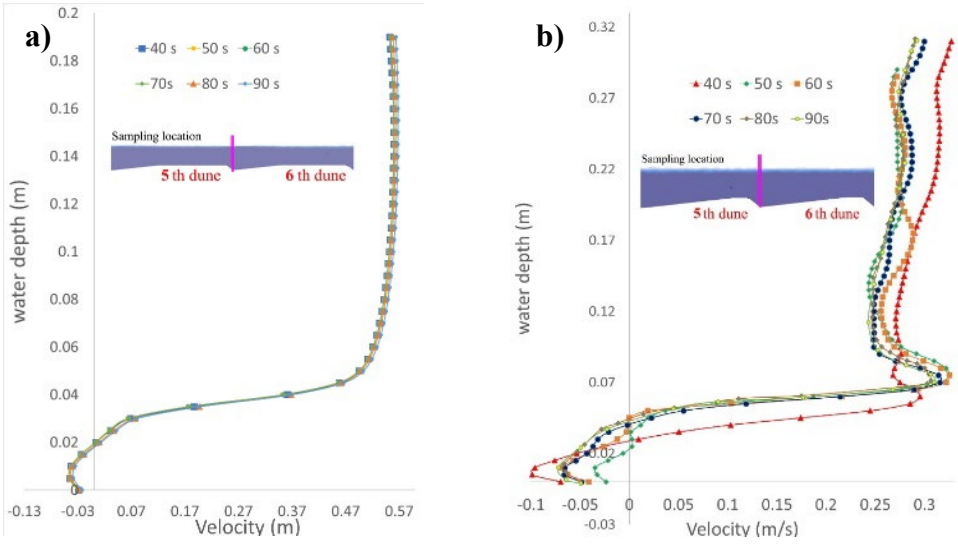

Figure 8. Flow velocity profiles at a distance of 7 meters of upstream at different times

2.7. Numerical model calibration

Twenty-nine experiments were simulated to evaluate the model by the measured velocity profiles in the vertical direction. The data of 11 experiments from Motamedi *et al.* (2012) (simulations No. 1, 2, 6, 7, 15, 21, 22, 23, 25, 26, 27) and one experiment from Balachandar and Patel (2008) (simulation No. 29 (Dune type 5, 18 mm grain size, 30 l/s flow rate and 120 mm flow depth)) were available. In all experiments, equation (4) was used to work

out the percentage error of the velocity profile of the numerical model (Num) relative to the measured laboratory data (Obs).

$$PercentofError(\%) = \frac{\sum_{i=1}^{n}(Obs-Num)}{\sum_{i=1}^{n}(Obs)} \times 100 \quad (4)$$

Where Obs = measured laboratory data and Num = numerical model output.

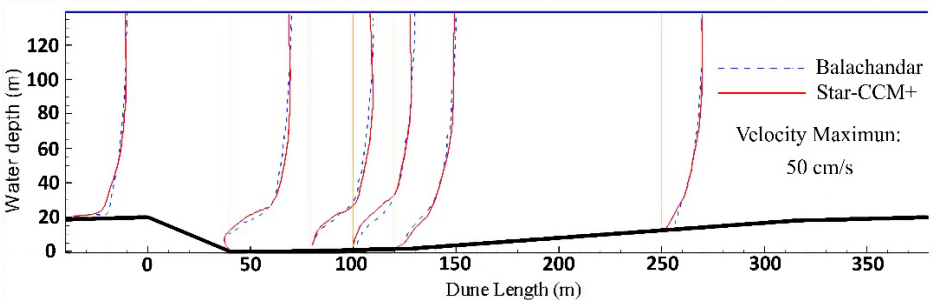

Figure 9. Comparative graph of flow velocity profiles in Experiment 29 (RANS turbulence model, Balachandar 2008 model geometry with a discharge of 36.7 litres per second and a 14 cm depth)

The results of the numerical model state that the difference between the predicted and measured values of the velocity profiles is on average 12.3% with Motamedi *et al.* (2012) and about 7.4% with Balachandar and Patel (2008) data. In total, the minimum and maximum differences are 7.4 and 16.8%, respectively, while the average is 11.9%, which highlights the appropriate agreement of the results of the present study with the previous research works (Figures 9 and Table 4).

Table 4. The average difference of vertical velocity profiles (%)

Simulation Number	1	2	6	7	15	21	22	23	25	26	27	29	Average
Observed and STAR-CCM+	11.4	9.5	13.2	15.5	14.5	9.4	10.2	16.8	12.2	9.6	12.8	7.4	11.9
STAR-CCM+ and SSIIM	21.6	18.9	23.2	26.5	17.3	15.2	14.1	24.5	19.3	13.2	27.7	-	20.1

The results of the STAR-CCM+ were also compared with the SSIIM used by Motamedi *et al.* (2012) study for simulation No. 15 (Dune type 3, 132 mm grain size, 30 l/s flow rate and 317 mm flow depth) (Figure 10). The minimum and maximum differences between the results of the predictions by the two models are 13.2 and 27.7%, respectively, with an average of about 20.1%. Bearing in mind that there is no information available for Balachandar *and* Patel (2008) data in SSIIM.

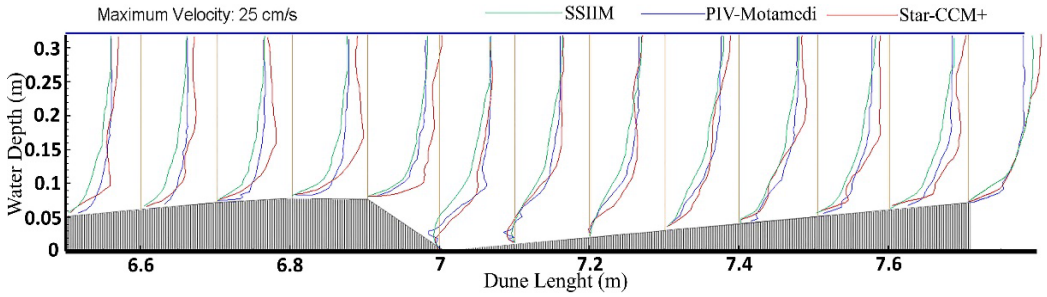

Figure 10. Comparative graph of flow velocity profiles in Experiment 15 (DES turbulence model, dune type 3 and 30 litres per second discharge and 32 cm depth)

3. Dimensional analysis

Given the significance of various variables in the formation of the bedform, it is possible to apply dimensional analysis to make these variables dimensionless. Generally, numerous variables are involved in developing the bedform, which are as follows.

$$f(V_*, H, \overline{V}, g, \mu, \rho, \rho_s, k_s, \lambda, \theta_{US}, \theta_{DS}, y, S, b, V_c, y_c) = 0 \quad (5)$$

Where V_* = shear velocity, H= dune height, D_{50} = median particle size, $\overline{V}$= mean flow velocity, g = gravity acceleration, μ= dynamic viscosity, ρ= water density, ρ_s= bed particle density, k_s= equivalent roughness height, λ = dune length, θ_{US} = dune stoss-side angle, θ_{DS}= dune lee-side angle, y = water depth, S = bed slope, τ_0= shear stress, b = channel width, V_c= critical velocity for particle movement, and y_c= critical depth for particle movement.

Totally, 18 variables are defined to form the dune, among which three repetitive variables are designated (i. e. H for the length, $\overline{V}$for the time and ρ for the mass).

Among the 29 available simulations, about 60% of them (i. e. 17 simulations) were used to obtain the coefficients of equation (6) while the remainders were for equation validation. The coefficients of the equation were calculated regression analyses with the coefficient of determination of$R^2 = 0.847$.

$$\frac{\lambda}{H} = 1.47\theta_{us}^{-0.023}\theta_{ds}^{-0.089}(Fr^2)^{-0.072}\left(\frac{k_s}{y}\right)^{0.032}\left(\frac{V_*}{\overline{V}}\right)^{-1.188} \quad (6)$$

Furthermore, the rest of the data (i. e. 12 simulations) were used to validate equation (6). The$\frac{\lambda}{H}$ values obtained by Equation (6) have an average percentage error of about 11.25% compared to the observed values (Figure 11).

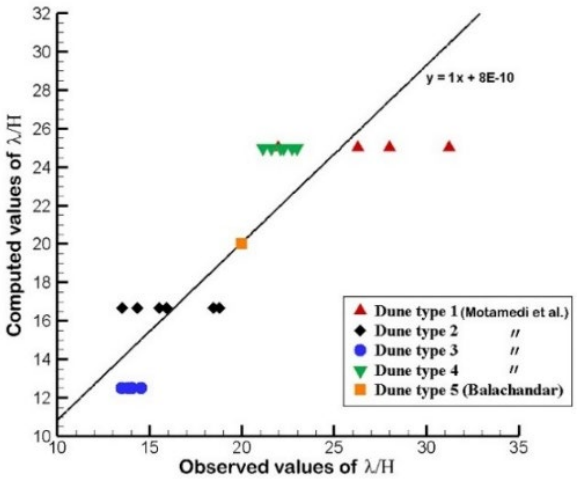

Figure 11. Comparison of the ratio of length to height observed and calculated according to equation (6)

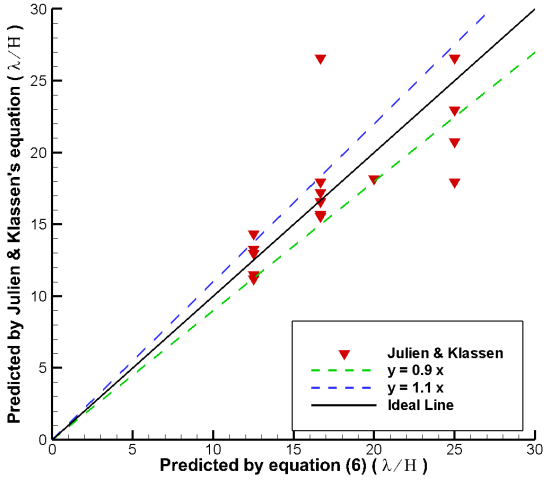

Figure 12. Comparison of λ/H values predicted by this study and Julien and Klassen 1995

Figure (12) provides the diagram of $\frac{\lambda}{H}$ values predicted by equation (6) versus those predicted by Julien and Klassen (1995). It is observed that the graphs are relatively symmetric for $\frac{\lambda}{H}$ values smaller than 20. In contrast, Equation (6) underestimates $\frac{\lambda}{H}$ values significantly for $\frac{\lambda}{H}$> 20 compared to Julien and Klassen (1995) equation with the average MND equals to 11.2.

3.1. Sensitivity analysis of the dimensionless numbers

Some researchers have used different variables to obtain the$\frac{\lambda}{H}$ ratio (Heydari *et al.* 2014; Attar and Li 2012; Karamisheva *et al.* 2005 and Julien and Klaassen 1995). This indicates that all dimensionless numbers in equation (6) may not necessarily appear in the equations developed by different researchers, as most studies have been carried out under controlled experimental conditions (Kwoll *et al.* 2016; Heydari *et al.* 2014 and Karamisheva *et al.* 2005). By conducting sensitivity analysis on each dimensionless number in equation (6), it is possible to conceive the significance of the numbers and their effects on estimating the dimensions of bedform and flow structure, which enables us to predict and control floods or probably to improve river ecosystem conditions (Naqshband and Hoitink 2020).

The sensitivity analysis was undertaken on dimensionless numbers of equation (6) for five different cases, such that, in each case, one dimensionless number was removed from the equation and the regression analysis was done to the data based on other dimensionless numbers (Table 5).

Table 5. Dependence of equation (13) dimensionless numbers

Deleted parameter	Formula	R^2	Percentage of deviation (MNE)
$\frac{k_s}{y}$	$\frac{\lambda}{H}=2.54\theta_{us}^{0.326}\theta_{ds}^{-0.087}(Fr^2)^{-0.06}\left(\frac{V_*}{V}\right)^{-1.168}$	0.837	9.6
$\frac{V_*}{V}$	$\frac{\lambda}{H}=19.22\theta_{us}^{0.98}\theta_{ds}^{-0.036}(Fr^2)^{-0.016}\left(\frac{k_s}{y}\right)^{0.036}$	0.03	26.2
Fr^2	$\frac{\lambda}{H}=3.29\theta_{us}^{0.287}\theta_{ds}^{-0.095}\left(\frac{k_s}{y}\right)^{0.001}\left(\frac{V_*}{V}\right)^{-1.118}$	0.78	11
θ_{DS}	$\frac{\lambda}{H}=2.49\theta_{us}^{0.24}(Fr^2)^{0.0236}\left(\frac{k_s}{y}\right)^{-0.076}\left(\frac{V_*}{V}\right)^{-1.137}$	0.786	10.8
θ_{US}	$\frac{\lambda}{H}=1.52\theta_{ds}^{0.32}(Fr^2)^{-0.089}\left(\frac{k_s}{y}\right)^{-0.072}\left(\frac{V_*}{V}\right)^{-1.188}$	0.84	9.4

Table (5) displays that the ratio $\frac{V_*}{V}$ has the most significant effect on equation (6) as a result of which the shear velocity and hence shear stress has the highest effect on riverbed formation which is in conformance with Willett (2006).

4. Conclusion

Generally, the use of computer simulations to model and study flows can reduce cost and time. In this research, the numerical model was used to simulate the dune geometry. Then, the experimental results of Motamedi *et al.* (2012) and Balachandar and Patel (2008) were used to validate the model. The comparison of the two vertical velocity profiles showed an average difference of 11.9%, which indicates the appropriate accuracy of the numerical model. Flow structure was also simulated numerically on five different types of dunes, the results of which are as follows:

-There is a high possibility of flow separation occurrence in sharp-crested dunes. In two dunes with the same dimensions, the sharp-crested dunes create more changes in the flow structure. However, shear stress variations in flat-crested dunes are more gradual than those of the sharp-crested dunes; therefore, flow separation is less likely to occur.

-The results of flow simulation with the RANS model state that the model works only for small-scale dunes to simulate flow separation zone. In contrast, LES and DES models detect flow separation with adequate accuracy near large-scale dunes, whereas they cause relatively intensive and irregular turbulences in small-scale dunes. The difference between LES and DES models could be noticeable in the generation of irregular vortices by LES in the flow layers away from the dunes and the lower DES run time. In other words, RANS and DES are the most appropriate turbulence models in simulating small and large-scale dunes, respectively.

-The results have revealed that the proposed equation (Equation 6) has a reasonable accuracy due to the random nature of the bedforms formation, in which the $\frac{V_*}{V}$ ratio has the most significant effect. Therefore, changing that may allow making changes in the characteristics related to the river bedforms.

5. REFERENCES

Aberle, J., Dittrich, A., Nestmann, F., Novak, P., Rennie, C. D., & Millar, R. G. (1999). Estimation of gravel-bed river flow resistance. *Journal of Hydraulic Engineering*, *125*(12), 1315–1319.

Ahmad, N., Saiful Bahry, S., Md Ali, Z., Mat Daud, A. and Musa, S. (2017). “Effect of Flow Resistance In Open Rectangular Channel”. MATEC Web of Conferences, 97, p.01107.

Alfonsi, G. (2009). “Reynolds-averaged Navier-Stokes equations for turbulence modelling”, Appl. Mech. Rev.,vol.62,pp. 040802.

Allen, J. R. L. (1985). “Principles of Physical Sedimentology”. Chapman and Hall, PP. 272

Allen, J.R.L. (1978). “Computational methods for dune time-lag: Calculations using Stein's rule for dune height”. Sedimentary Geology 20(3): 165-216.

Attar, S. and Li, S.S. (2012). “Numerical investigation of flow structure and shear stress over fixed dunes”. International Conference on Fluvial Hydraulics River Flow 2012, San José, Costa Rica, 5–7 September 2012.

Balachandar, R., and Patel, V.(2008). “Flow over a fixed rough dune”. Canadian Journal of Civil Engineering, 35(5), pp.511-520.

Berrouk, A. (2019). “Stochastic Lagrangian modeling for large eddy simulation of dispersed turbulent two-phase flows”. Bentham Science Publishers, p 23.

Bunge, U., Mockett C., and Thiele F. (2007). “Guidelines for implementing Detached-Eddy Simulation using different models”. Aerospace Science and Technology, Vol. 11, pp. 376-385.

Cai, R., Zhang, H., Zhang, Y., Zhang, L. and Huang, H. (2020). “Flow Resistance Equation in Sand-bed Rivers and Its Practical Application in the Yellow River”. Water, 12(3), p.727.

Chow, V.T. (1981). “Open channel hydraulics”. Mc Graw – Hill Limted, London, 680 p.

DavarPanah, Sh. (2011). “Investigation of Interaction of Straight Crested Gravel Bedforms and Vegetated Banks on Turbulent Flow Components”, Master’s Thesis, Faculty of Agriculture, Isfahan University of Technology, Isfahan, Iran. (in Persian)

Engelund, F., and Hansen, E.(1967). “A Monograph on Sediment Transport in Alluvial Streams”. Teknisk Vorlag, Copenhagen, Denmark.

Fenton, J.D. (2010). “Calculating resistance to flow in open channels”. Alternative Hydraulics Paper, 2, 1-7.

Gilbert, G. K.(1914). “The transition of debris by running water”. U.S. Geol. Surv. Prof. Pap. 86, pp 263.

Giri, S. and Shimizu, Y., (2006). Numerical computation of sand dune migration with free surface flow. Water Resources Research, 42(10).

Hafez, Y.I., El-Gamal, F.S., and Soliman, W.R. (2001). “River Nile bed forms, resistance to flow and discharge prediction”. Water Science, the 28th – 29th issue, October 2000-April 2001.

Heydari, H., Zarrati, A.R., and Karimaee Tabarestani, M. (2014). “Bedform characteristics in alive bed alluvial channel”. Scientia Iranica,TransactionsA:CivilEngi- neering, 21(6), 1773–1780.

Hirt, C.W. and Nichols, B.D. (1981). “Volume of Fluid (VOF) Method for the Dynamics of Free Boundaries”. Journal of Computational Physics, 39, 201-225.

Ji-Sung, K., Chan-Joo, L., Won, K. and Yong-Jeon, K., (2010). Roughness coefficient and its uncertainty in gravel-bed river. *Water Science and Engineering*, 3(2).

Julien, P.Y., and Klaassen, G.J. (1995). “Sand-dune geometry of large rivers during floods”. Journal of Hydraulic Engineering, 121, 657-663.

Karamisheva, R., Lyness, J. F., Myers W. R. C., O'Sullivan J. and Cassells J. (2005). “Prediction of bed form height in straight and meandering compound channels”. Proceedings of the 3rd International Conference on Water Resources Management, Algarve, Portugal, 11-13 April, 311-320.

Kwoll, E., Venditti, J.G., Bradley RW, Winter C. (2016). “Flow structure and resistance over subaqueous high- and low-angle dunes”. Journal of Geophysical Research: Earth Surface 121(3): 545–564.

Lefebvre, Alice. (2019). “Three-Dimensional Flow Above River Bedforms: Insights From Numerical Modeling of a Natural Dune Field (Río Paraná, Argentina)”. Journal Of Geophysical Research: Earth Surface, 124(8) 2241-2264.

Maddux, T. B., Nelson, J. M., & McLean, S. R. (2003). “Turbulent flow over three-dimensional dunes: 1. Free surface and flow response”. Journal of Geophysical Research: Earth Surface, 108(F1).

Motamedi, A., Afzalimehr, H. Singh, V., and Dufresne, L.(2012). “Experimental Study on the Influence of Dune Dimensions on Flow Separation”. Journal of Hydrologic Engineering, 19(1), pp.78-86.

Mustaffa, N., Ahmad, N., and Razi, M. (2016). “Variations of Roughness Coefficients with Flow Depth of Grassed Swale”. IOP Conference Series: Materials Science And Engineering, 136, 012082.

Naqshband, S. and Hoitink, A. (2020). “Scale-Dependent Evanescence of River Dunes During Discharge Extremes”. Geophysical Research Letters, 47(6).

Nasiri DehSorkhi, A. (2010). “Interaction of vegetation cover, bed forms and flow structure on distributions of velocity and turbulent intensities”. Master’s Thesis, Faculty of Agriculture, Isfahan University of Technology, Isfahan, Iran. (In Persian)

Nabi, M., de Vriend, H., Mosselman, E., Sloff, C. and Shimizu, Y., (2012). Detailed simulation of morphodynamics: 1. Hydrodynamic model. *Water Resources Research*, 48(12).

Nelson, J. M., McLean, R. and Wolfe,S. (1993). "Mean flow and turbulence over fixed, two-dimensional bed form. Water Resour. Res. 29: 3935-3953.

Niazkar, M., Talebbeydokhti, N., and Afzali, S. (2019). "Development of a New Flow-dependent Scheme for Calculating Grain and Form Roughness Coefficients". KSCE Journal Of Civil Engineering, 23(5), pp 2108-2116.

Park, J., Kim, B., Sohn, D., Choi, Y. and Lee, Y. (2020). "A Study on Flow Characteristics and Flow Uniformity for the Efficient Design of a Flow Frame in a Redox Flow Battery". Applied Sciences, 10(3), p.929.

Parsons, D. R., Best, J. L., Orfeo, O., Hardy, R. J., Kostaschuk, R., and Lane, S. N. (2005). "Morphology and flow fields of three-dimensional dunes, Rio Paraná, Argentina: results from simultaneous multibeam echo sounding and acoustic Doppler current profiling". Journal of Geophysical Research, 110(F4), F04S03.

Reisenbüchler, M., Bui, M., Skublics, D., and Rutschmann, P. (2019). "An integrated approach for investigating the correlation between floods and river morphology: A case study of the Saalach River, Germany". Science Of The Total Environment, Vol. 647, pp 814-826.

Shur, M., Spalart P.R., Strelets M., and Travin A. (1999). "Detached-eddy simulation of an airfoil at highangle of attack". Engineering Turbulence Modeling and Experiments, Vol. 4, pp. 669-678.

Soulsby, R. L. (1989). "Bedform migration in sandy estuaries". H.R Wallingford Res. Rep. No. SR 208, pp 16.

Spalart, P. R., Jou, W.-H., Strelets, M., and Allmaras, S. R. (1997). "Comments on the Feasibility of LES for Wings, and on a Hybrid RANS/LES Approach". Proceedings of the First ASOSR Conference on DNS/LES, Greyden Press, Columbus, OH.

Strickler, A. (1923). "Some contributions to the problem of the velocity formula and roughnessfactors for rivers, canals, and closed conduits". Bern, Switzerland, Mitt.Eidgeno assischen Amtes Wasserwirtschaft, no. 16.

Van Mierlo, M. C. L. M. and de Ruiter, J. C. C. (1988). "Turbulence measurements above artificial dunes, Report on measurements". Report Q789, WL | Delf Hydraulic, Delf, The Nederlands.

Van Rijn, L.C. (1984c). "Sediment Transport, Part III: Bed Forms and Alluvial Roughness". Journal of Hydraulic Engineering, ASCE, Vol. 110, No. 12.

Venditi, J. G. (2007). "Turbulent flow and drag over fixed two- and three-dimensional dunes". J. Geophys. Res. 112 F04008.

Willett, S. (2006). "Tectonics, Climate, And Landscape Evolution. Boulder, Colo". Geological Soc. of America, pp.83-84.